



HORIZON 2020



# Product Traceability and Uncertainty for the EARLINET LIDAR aerosol extinction coefficient product

**Version 0.4**

*GAIA-CLIM  
Gap Analysis for Integrated  
Atmospheric ECV Climate Monitoring  
Mar 2015 - Feb 2018*

**A Horizon 2020 project; Grant agreement: 640276**

**Date: 23 January 2018**

**Dissemination level: PU**

*Work Package 2; Compiled by Marco Rosoldi &  
Fabio Madonna (CNR-IMAA)*



## Table of Contents

Table of Contents .....	2
1 Product overview .....	3
2 Introduction.....	3
3 Instrument description .....	4
4 Product Traceability Chain .....	7
5 Element contributions .....	8
5.1 Transmission system (1) .....	8
5.2 Receiving system (2).....	9
5.3 Receiver optical parameters (2a).....	9
5.4 Alignment of the lidar system (2b) .....	10
5.5 Detectors (3).....	12
5.6 Acquisition (4) .....	13
5.7 Raw Raman signals (5) .....	14
5.8 Pre-processing of Raman signals (6) .....	15
5.9 Dead Time correction (6a) .....	16
5.10 Dark subtraction (6b) .....	18
5.11 First range bin/Trigger delay (6c) .....	19
5.12 Background subtraction (6d).....	21
5.13 Vertical integration (binning) (6e) .....	22
5.14 Temporal integration (6f).....	23
5.15 Signal gluing (6g).....	24
5.16 Overlap Correction (6h) .....	27
5.17 Processing of Raman signals (7).....	28
5.18 Molecular density and extinction profiles (7a) .....	29
5.19 Angstrom exponent assumption (7b) .....	31
5.20 Multiple scattering correction (7c).....	32
5.21 Retrieval of aerosol extinction coefficient profile (7d).....	33
6 Uncertainty Summary .....	35
7 Traceability uncertainty analysis .....	38
7.1 Recommendations .....	39
8 Conclusion .....	40
9 References.....	40

## 1 Product overview

Product name: EARLINET LIDAR aerosol extinction coefficient

Product technique: LIDAR

Product measurand: Aerosol extinction coefficient

Product form/range: profile/from full overlap altitude (250-500 m above the ground, depending on the instrument) to 12 km

Product dataset: EARLINET Database

Site/Sites/Network location:

- Evora, Portugal, 38.568 °N, 7.912 °W, 293 m
- Granada, Spain, 37.164 °N, 3.605 °W, 680 m
- Leipzig, Germany, 51.353 °N, 12.435 °E, 90 m
- Napoli, Italy, 40.8380 °N, 14.1830 °E, 118 m
- Potenza, Italy, 40.601 °N, 15.724 °E, 760 m

Product time period: June 1, 2006 – December 31, 2010

Data provider: CNR-IMAA

Instrument provider: EARLINET lidar stations

Product assessor: Fabio Madonna, CNR-IMAA

Assessor contact email: fabio.madonna@imaa.cnr.it

## 2 Introduction

This document presents the Product Traceability and Uncertainty (PTU) information for the EARLINET LIDAR aerosol extinction coefficient product. The aim of this document is to provide supporting information for the users of this product within the GAIA-CLIM VO. The uncertainty and traceability information contained in this document is based on the references reported at the end of the document.

The advanced network of ground-based lidar stations EARLINET (European Aerosol Research Lidar NETwork) has been operating for more than 15 years and currently consists of 31 measuring stations located in Europe, running different lidar systems and processing algorithms [1]. The EARLINET community has developed over the years robust lidar data processing algorithms to retrieve the vertical profiles of aerosol extinction coefficient in the troposphere and lower stratosphere, with a sampling time ranging from a few tens of minutes to a few hours and a vertical resolution ranging from a few hundreds of meters to many hundreds of meters, depending on the observed atmospheric scenario and the lidar system. Currently, the network is developing a rigorous quality assurance program addressing both instrument performance and evaluation of the algorithms to ensure instrument standardization and consistent lidar retrievals within the network using a common data format. For the full harmonization of data analysis and data traceability, the EARLINET Single Calculus Chain (SCC) [2,3], a tool for the automatic quality assured analysis of lidar measurements, has been developed.

The major part of the measurements is performed according to a fixed schedule three times a week: two measurements after sunset, on Monday and Thursday, and one measurement around noon (local time) on Monday. This permits an unbiased statistically significant data set. Additional measurements are performed to address specific events that are localized either in space or time (e.g., forest fires, volcanic eruptions, desert dust outbreaks). Since June 2006, EARLINET stations have been

performing measurements during the overpasses of the NASA CALIPSO satellite, launched in April 2006, in order to validate and calibrate the satellite lidar products [4].

EARLINET algorithms include the estimation of the random uncertainty and a separate estimation of the systematic uncertainties due to the retrieval assumptions, background models, and corrections implemented in a typical lidar data processing chain. For the retrieval of aerosol extinction coefficient at 532 nm, available only from night time measurements, random uncertainty estimates are typically less than 10% for values higher than  $2 \times 10^{-5} \text{ m}^{-1}$  and greater for lower extinction coefficient values (see sub-section 5.21). On the other hand, the estimates of systematic uncertainty due to each contribution are less than 10%, resulting in a total maximum systematic uncertainty less than 15% for extinction coefficient values higher than  $2 \times 10^{-5} \text{ m}^{-1}$  and for all the altitude levels above the full overlap altitude of the lidar system (see sub-section 5.1 and following sub-sections).

A comprehensive strategy for campaign setup and data evaluation has been established at the European level [5]. Eleven systems from nine EARLINET stations participated in the EARLINET Lidar Intercomparison 2009 (EARLI09) measurement campaign. In this campaign, three reference systems were qualified to serve as travelling standards thereafter. Eleven EARLINET systems from ten other stations have been compared against these reference systems since 2009; afterwards these systems have calibrated other instruments moving from their own station to the other sites in the various countries.

Currently, a strategy for ensuring the lidar system comparability at a global scale is missing. GALION (GAW Lidar Observation Network) is the global federation of lidar networks operating globally: the network implementation is challenging and its collective operation is limited to special events like volcanic eruptions [6]. Nevertheless, the lidar calibration facility (LICAL), undertaken by the ACTRIS-2 H2020 research infrastructure project, offers to calibrate all lidar system types from outside the ACTRIS community with a special focus on GALION federated networks. In future LICAL could become the calibration centre for the global lidar network.

### 3 Instrument description

The basic setup of a lidar system is shown in figure 1. Lidar technique, acronym for "light detection and ranging", is based on the transmission into the atmosphere of short light pulses, with duration ranging from a few to several hundreds of nanoseconds, by a laser transmitter, directly or by means of transmission optics (e.g. beam expander), depending on the lidar system. In any point of the atmospheric volume crossed by the laser beam, a portion of the incident light is backscattered towards the transmitter by atmospheric constituents. This light backscattered by the atmosphere at different distances from the transmitter is collected by a telescope and passes through an optical system, consisting of various elements (lenses, mirrors, filters etc.), which selects specific wavelengths or polarization states of the light collected by the telescope and whose configuration depends on the particular lidar system. The light from the optical system is forwarded to detectors, typically photomultiplier tubes, which convert it into electrical signals.

An electronic circuit (trigger) allows to synchronize the acquisition start with the emission of each laser pulse so that the electrical signals are acquired as a function of elapsed time with respect to the emission of each laser pulse. As this is the time that the light pulse takes to travel from the transmitter to the backscatter point and vice versa, then, due to the constant speed of light, it is possible to calculate the distance between the transmitter and the backscatter point and convert electrical signals acquired as a function of time into signals as a function of that distance. These are the lidar signals,

measuring the intensity of the light backscattered by the atmosphere as a function of the distance from the lidar.

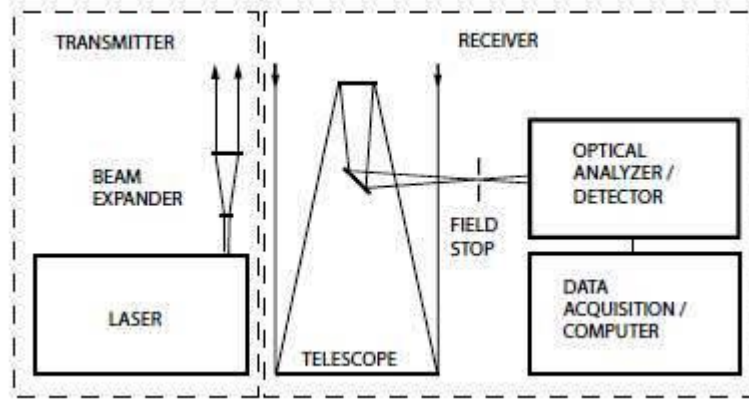


Figure 1: Principle setup of a lidar system

More specifically, the basic equation for the analysis of lidar signals (the lidar equation) describes the intensity of the measured signals depending on the distance from the lidar, several instrumental parameters and atmospheric properties. In order to retrieve the atmospheric parameters, the lidar equation needs to be inverted in the approximation of single and independent scattering. This means that a photon is scattered only once by the atmospheric constituents and that the scatterers are well separated and randomly moving. Thus, the contributions to the total scattered energy by many targets have no phase relation and the total intensity is simply the sum of the intensities scattered from each target. In this approximation, the lidar equation, in a general form, can be written as:

$$P(\lambda_L, \lambda_S, z) = P_L \frac{c \tau_d}{2} \frac{A}{z^2} \Psi(\lambda_S, \lambda_L) O(z) \beta(\lambda_S, \lambda_L, z) T(\lambda_L, z) T(\lambda_S, z) + P_B \quad (1)$$

where:

- $P(\lambda_L, \lambda_S, z)$  is the received optical power from the distance  $z$  at a specific polarization and wavelength  $\lambda_S$ , due to the backscattering of the laser wavelength  $\lambda_L$ .  $P_L$  is the mean power of a single laser pulse.  $c \tau_d / 2$  represents the lidar vertical resolution, where  $c$  and  $\tau_d$  are respectively the light speed and the dwell time, that is the time resolution or the sampling time of the acquisition system, whose minimum value is the duration of a laser pulse.  $A/z^2$  is the acceptance solid angle of the telescope for light scattered at distance  $z$ , which represents the probability that a photon scattered at the distance  $z$  is collected by the receiving telescope of area  $A$ .
- $\Psi(\lambda_S, \lambda_L) = \xi(\lambda_L, \lambda_S) \eta(\lambda_S)$  is the overall system efficiency, where  $\xi(\lambda_L, \lambda_S)$  is the optical efficiency, including the reflectivity and transmissivity of all the optics encountered both by the transmitted and the received light (lenses, mirrors, filters etc.), while  $\eta(\lambda_S)$  is the quantum efficiency of the detector.  $O(z)$  is the lidar overlap function, depending on the lidar geometry, that describes the incomplete overlap between the emitted laser beam and the receiver field of view close to the lidar.  $O(z)$  ranges between 0, for  $z = 0$ , and 1, above a certain height  $z_{ovl}$ , called full overlap height, where the laser beam is completely imaged onto the detector and the overlap is complete.
- $\beta(\lambda_S, \lambda_L, z)$  is the atmospheric backscatter coefficient at the wavelength  $\lambda_S$  and distance  $z$ ; for elastic lidar signals, due to the elastic backscattering of laser pulses ( $\lambda_S = \lambda_L$ ) by atmospheric

molecules and particles (aerosol and clouds), the backscatter coefficient is the sum of two contributions, the molecular and particle backscatter coefficients; for Raman lidar signals, due to the Raman inelastic backscattering of laser pulses ( $\lambda_S \neq \lambda_L$ ) by atmospheric molecules (due to the transitions of roto-vibrational or purely rotational Raman spectra of these molecules), the backscatter coefficient has only the molecular contribution.

- $T(\lambda_L, z)$  and  $T(\lambda_S, z)$  are the atmospheric transmissivities for the laser light at wavelength  $\lambda_L$  on the way from the laser source to the distance  $z$  and for the backscattered light at wavelength  $\lambda_S$  on the way from the distance  $z$  to the receiver; these terms can be expressed as:

$$T(\lambda_L, z) = \exp\left(-\int_0^z \alpha_{\lambda_L}(z')dz'\right) \quad \text{and} \quad T(\lambda_S, z) = \exp\left(-\int_0^z \alpha_{\lambda_S}(z')dz'\right) \quad (2)$$

where  $\alpha_{\lambda_L}(z)$  and  $\alpha_{\lambda_S}(z)$  are the atmospheric extinction coefficients at wavelengths  $\lambda_L$  and  $\lambda_S$  at distance  $z$ . As extinction can occur because of scattering and absorption of light by molecules and particles, the above extinction coefficients can be expressed as the sum of four components, the scattering and absorption coefficients of molecules and the scattering and absorption coefficients of particles (aerosol and clouds).

- $P_B$  is the background contribution to the received power of the lidar signal, in addition to the contribution due to the portion of the laser beam backscattered by the atmosphere. The background signal is generated by the detector noise and, at daytime, by direct or scattered sunlight, at nighttime, by the moon, the stars as well as artificial light sources.

Typically, EARLINET lidars transmit light pulses at 355, 532 and 1064 nm and receive the elastically backscattered light from the atmosphere at the same wavelengths and the Raman inelastically backscattered light from atmospheric nitrogen molecules at 387 and 607 nm. The atmospheric profiles of aerosol extinction coefficient at 532 (355) nm are retrieved by EARLINET algorithms, using the nitrogen Raman signals at 607 (387) nm. These signals are not affected by the aerosol backscattering, as only a specific molecular species can backscatter inelastically at the corresponding Raman wavelength. As a consequence, the contribution of the aerosol in the Raman signals is confined only in the transmissivity terms, where both molecular and aerosol extinction coefficients play a role. Therefore, if backscatter and extinction coefficients of molecules are known, it is possible to solve the lidar equation (1) to retrieve the aerosol extinction coefficient.

The profile of aerosol extinction coefficient at  $\lambda_L = 532\text{nm}$  is directly derived from the pre-processed Raman signals at  $\lambda_S = 607\text{nm}$  by the following equation [23,24]:

$$\alpha_{\lambda_L}^{par}(z) = \frac{\frac{d}{dz}\{\ln[N(z)/P_{\lambda_S}(z)z^2]\} - \alpha_{\lambda_L}^{mol}(z) - \alpha_{\lambda_S}^{mol}(z)}{1 + (\lambda_L/\lambda_S)^{\mathring{a}}} \quad (3)$$

where:  $\alpha_{\lambda_L}^{par}(z)$  is the particle extinction coefficient at the wavelength  $\lambda_L$  and range  $z$ ;  $P_{\lambda_S}(z)$  is the power of the pre-processed Raman signal at wavelength  $\lambda_S$  and range  $z$ ;  $N(z)$  is the number density of atmospheric nitrogen molecules at range  $z$ ;  $\alpha_{\lambda_L}^{mol}(z)$  and  $\alpha_{\lambda_S}^{mol}(z)$  are the molecular extinction coefficients at wavelengths  $\lambda_L$  and  $\lambda_S$ , respectively;  $\mathring{a}$  is the Ångström exponent, that describes the wavelength dependence of particle extinction coefficient. It is defined by the following relation:

$$\frac{\alpha_{\lambda_L}^{par}(z)}{\alpha_{\lambda_S}^{par}(z)} = \left(\frac{\lambda_S}{\lambda_L}\right)^{\mathring{a}} \quad (4)$$

## 4 Product Traceability Chain

Figure 2 shows the traceability chain for atmospheric profile of aerosol extinction coefficient retrieved with Raman lidar technique within EARLINET network. The chain has been developed following the approach outlined in the Guide to Uncertainty in Measurement & its Nomenclature, published as part of the GAIA-CLIM project.

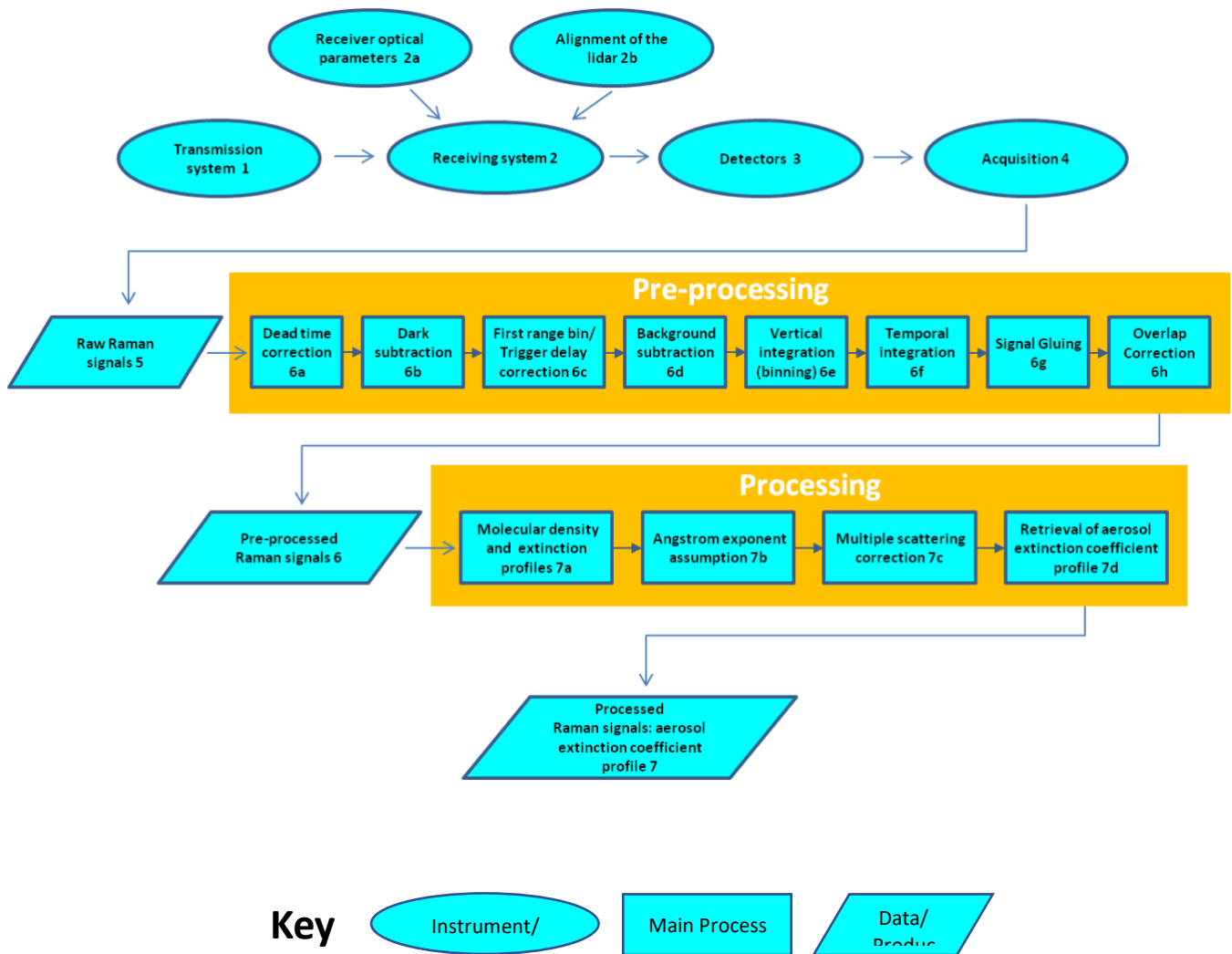


Figure 2: Traceability chain for atmospheric profile of aerosol extinction coefficient retrieved with Raman lidar technique within EARLINET network

## 5 Element contributions

### 5.1 Transmission system (1)

Light pulses at wavelength  $\lambda_L = 532nm$  are sent out into the atmosphere by a laser transmitter, directly or by means of transmission optics (e.g.: beam expander, mirrors etc.) depending on the lidar system. The parameters of the laser transmitter (pulse duration, energy and repetition rate, beam diameter and divergence) as well as of the transmission optics change depending on the lidar system. Additionally, such parameters may also change for a given lidar system due to their time and temperature instability or to the replacement of one or more components of the transmission system. These variations affect the optical power transmitted in the atmosphere and therefore both the power and the random uncertainty of the Raman signals at  $\lambda_S = 607nm$  used in the algorithms for the retrieval of aerosol extinction coefficient profile. However, at EARLINET lidar stations these variations are monitored and minimized (e.g., pulse energy is measured before each measurement session, lidars usually operate in air-conditioned environments), so that their contribution to the retrieval and uncertainty of aerosol extinction coefficient profile is assumed to be negligible.

Information / data	Type / value / equation	Notes / description
<b>Name of effect</b>	Transmission system	Contribution of variations in all the parameters related to the laser beam transmission to the atmosphere.
<b>Contribution identifier</b>	1	
<b>Measurement equation parameter(s) subject to effect</b>	$P_L$ and $\xi(\lambda_L, \lambda_S)$ in lidar equation of Raman signals at $\lambda_S = 607nm$	
<b>Contribution subject to effect (final product or sub-tree intermediate product)</b>	Aerosol extinction coefficient profile $\alpha(z)$	
<b>Time correlation extent &amp; form</b>	Various time scales	Extent & form not quantified
<b>Other (non-time) correlation extent &amp; form</b>	1) Possible correlation with vertical range (if pulse duration increases so as to exceed the dwell time); 2) Possible correlation with the temperature of laser and transmission optics during measurements	Extent & form not quantified
<b>Uncertainty PDF shape</b>	N/A	Systematic effect
<b>Uncertainty &amp; units</b>	0% (relative uncertainty)	(Assumed to be negligible)
<b>Sensitivity coefficient</b>	< 1	(Assumed to be negligible)
<b>Correlation(s) between affected parameters</b>	None	
<b>Element/step common for all sites/users?</b>	Yes	
<b>Traceable to ...</b>	N/A	
<b>Validation</b>	N/A	

## 5.2 Receiving system (2)

The portion of the laser radiation backscattered by the atmosphere at different altitude ranges is collected by a telescope. Two or more telescopes with different optical properties can be used to optimize lidar performances in different atmospheric regions (near range, far range). The radiation collected by the telescope passes through an optical system (consisting of lenses, mirrors, filters, beam splitters and interference filters) where it is spectrally filtered, so as only the Raman backscattered light from atmospheric nitrogen molecules at wavelength  $\lambda_S = 607nm$  is transmitted to the detection system. The uncertainty contribution of the receiving system is the combination of contributions related to the receiver optical parameters (2a) and the alignment of the lidar system (2b), whose uncertainties and correlation effects are described in the corresponding sub-level sections.

Information / data	Type / value / equation	Notes / description
<b>Name of effect</b>	Receiving system	Combined contribution of the receiver optical parameters (2a) and alignment of the lidar system (2b)
<b>Contribution identifier</b>	2	
<b>Measurement equation parameter(s) subject to effect</b>	$O(z)$ and $\xi(\lambda_L, \lambda_S)$ in lidar equation of Raman signals at $\lambda_S = 607nm$	
<b>Contribution subject to effect (final product or sub-tree intermediate product)</b>	Aerosol extinction coefficient profile $\alpha(z)$	
<b>Time correlation extent &amp; form</b>	Various time scales	Extent & form not quantified
<b>Other (non-time) correlation extent &amp; form</b>	May affect vertical correlation	
<b>Uncertainty PDF shape</b>	N/A	Systematic effect
<b>Uncertainty &amp; units</b>	0% (relative uncertainty) combination of 2a and 2b	Assumed to be negligible
<b>Sensitivity coefficient</b>	1	
<b>Correlation(s) between affected parameters</b>	None	
<b>Element/step common for all sites/users?</b>	Yes	
<b>Traceable to ...</b>	N/A	
<b>Validation</b>	N/A	

## 5.3 Receiver optical parameters (2a)

The optical properties of the elements forming the receiver, consisting of the telescope and the following optical filtering system, change depending on the lidar system, but they may also change for a given lidar system due to their time and temperature instability, contamination, or to the replacement of one or more components of the receiving system. These variations in the parameters of the receiving system affect the optical power transmitted by the receiver to the detectors and therefore both the power and the random uncertainty of the Raman signals at  $\lambda_S = 607nm$  used in

the algorithms for the retrieval of aerosol extinction coefficient profile. However, at EARLINET lidar stations these variations are monitored and minimized (e.g., the optics are regularly cleaned, lidars usually operate in air-conditioned environments), so that their contribution to the retrieval and uncertainty of aerosol extinction coefficient profile is assumed to be negligible.

Information / data	Type / value / equation	Notes / description
<b>Name of effect</b>	Receiver optical parameters	Contribution of variations in all the optical parameters of the receiving system
<b>Contribution identifier</b>	2 a	
<b>Measurement equation parameter(s) subject to effect</b>	$\xi(\lambda_L, \lambda_S)$ in lidar equation of Raman signals at $\lambda_S = 607nm$	
<b>Contribution subject to effect (final product or sub-tree intermediate product)</b>	Aerosol extinction coefficient profile $\alpha(z)$	
<b>Time correlation extent &amp; form</b>	Various time scales	Extent & form not quantified
<b>Other (non-time) correlation extent &amp; form</b>	1) Possible correlation with vertical range due to the correlation of the optical efficiency of the receiving system with the incident angle of backscattered light and, consequently, with the vertical range; 2) Possible correlation with the temperature of the receiver components during measurements	Extent & form not quantified
<b>Uncertainty PDF shape</b>	N/A	Systematic effect
<b>Uncertainty &amp; units</b>	0% (relative uncertainty)	(Assumed to be negligible)
<b>Sensitivity coefficient</b>	< 1	(Assumed to be negligible)
<b>Correlation(s) between affected parameters</b>	None	
<b>Element/step common for all sites/users?</b>	Yes	
<b>Traceable to ...</b>	N/A	
<b>Validation</b>	N/A	

#### 5.4 Alignment of the lidar system (2b)

The correct alignment of the lidar system, that is the alignment of the laser beam with the receiving system and of the telescope with the optics of filtering system, is ensured by specific tests developed by the EARLINET quality assurance program. In particular, the telecover test and the Rayleigh fit

test are performed to check and correct the alignment of the lidar system in the near range (planetary boundary layer) and in the far range (free troposphere or above), respectively. A detailed description of these tests can be found in [7].

For each lidar system there is a certain degree of misalignment between the laser beam and the receiving system due to residual uncertainties in the telecover and Rayleigh fit tests or possible mechanical/thermal instabilities of the optical and mechanical components forming both transmission and receiving systems. The misalignment of a lidar system changes the incident angle on the receiver of the backscattered light at each altitude level, which affects both the overlap function and the optical power transmitted by the receiver to the detectors and, definitively, the power of the Raman signals at  $\lambda_S = 607nm$  used in the algorithms for the retrieval of aerosol extinction coefficient profile. At EARLINET stations the above quality assurance tests for the correct alignment of the lidar system are regularly performed, so that the contribution of the lidar misalignment to the uncertainty of aerosol extinction coefficient profile is assumed negligible.

Information / data	Type / value / equation	Notes / description
<b>Name of effect</b>	Alignment of the lidar system	Contribution of lidar misalignment
<b>Contribution identifier</b>	2b	
<b>Measurement equation parameter(s) subject to effect</b>	$O(z)$ and $\xi(\lambda_L, \lambda_S)$ in lidar equation of Raman signals at $\lambda_S = 607nm$	
<b>Contribution subject to effect (final product or sub-tree intermediate product)</b>	Aerosol extinction coefficient profile $\alpha(z)$	
<b>Time correlation extent &amp; form</b>	Various time scales	Extent & form not quantified
<b>Other (non-time) correlation extent &amp; form</b>	1) Possible correlation with vertical range due to the correlation of $O(z)$ and optical efficiency of the receiving system with the vertical range; 2) Possible correlation with the temperature of components forming both transmission and receiving systems during measurements	Extent & form not quantified
<b>Uncertainty PDF shape</b>	N/A	Systematic effect
<b>Uncertainty &amp; units</b>	0% (relative uncertainty)	Assumed to be negligible
<b>Sensitivity coefficient</b>	1	
<b>Correlation(s) between affected parameters</b>	None	
<b>Element/step common for all sites/users?</b>	Yes	
<b>Traceable to ...</b>	No	
<b>Validation</b>	No	

## 5.5 Detectors (3)

The Raman backscattered light at  $\lambda_S = 607\text{nm}$  from the filtering optical system is forwarded to detectors, consisting of photomultiplier tubes (PMTs), where it is converted to electrical signals. The main uncertainty contribution of the detectors is related to the spatial inhomogeneities of their photocathode, that is the variation of its sensitivity with the position of incident light on it. This can cause range dependent artifacts in Raman signals at  $\lambda_S = 607\text{nm}$ , because the backscattered light at different altitude levels is projected by the receiving system onto different areas of the photocathode characterized by different sensitivities. Therefore, the power of the Raman signals at  $\lambda_S = 607\text{nm}$  at different altitudes may change not only because of vertical distribution of atmospheric parameters, but also because of the variability with the altitude of detector quantum efficiency. The effects of PMT spatial inhomogeneities on lidar signals have been simulated in Simeonov et al. [8] and Freudenthaler [9], where optical configurations to minimize these effects are also described. With conventional optical configurations (direct illumination of the PMT), lidar signal deviations up to 90% have been calculated, which can result in very large systematic uncertainty in the retrieved aerosol extinction coefficient. This uncertainty, depending on the exact location of the lidar spots on the PMT, usually unknown, is unpredictable. With suitable optical setups before the PMT, consisting of field lens, optical diffusers, mirror tubes and optical fibers used alone or in combination, maximum deviations of lidar signals can be strongly reduced, ranging between 30% and 1%, depending on the optical setup used to imagine the telescope primary mirror on a small area of the PMT photocathode. Another uncertainty contribution of the detectors is related to the variations of their quantum efficiency due to their ageing. These variations also affect the power of the Raman signals at  $\lambda_S = 607\text{nm}$ .

For EARLINET lidars, equipped with suitable optical setups minimizing the effects of PMTs spatial inhomogeneities, the contribution of the detectors to the uncertainty of aerosol extinction coefficient profile is assumed negligible. In particular, the telecover test, regularly performed for the correct alignment of the lidar in the near range and described in [7], also allows to identify possible deviations in lidar signals due to the PMT inhomogeneities. In this case, the optical system before the PMT is optimized so as to minimize these deviations.

Information / data	Type / value / equation	Notes / description
<b>Name of effect</b>	Detectors	Contribution related to the efficiency of detectors
<b>Contribution identifier</b>	3	
<b>Measurement equation parameter(s) subject to effect</b>	$\eta(\lambda_S)$ in lidar equation of Raman signals at $\lambda_S = 607\text{nm}$	
<b>Contribution subject to effect (final product or sub-tree intermediate product)</b>	Aerosol extinction coefficient profile $\alpha(z)$	
<b>Time correlation extent &amp; form</b>	Various time scales	Extent & form not quantified
<b>Other (non-time) correlation extent &amp; form</b>	Correlation with vertical range due to the correlation with vertical range of the intensity distribution of the lidar spot on the PMT photocathode	Extent & form (depending on the particular lidar system) not quantified
<b>Uncertainty PDF shape</b>	N/A	Systematic effect

<b>Uncertainty &amp; units</b>	0% (relative uncertainty)	Assumed to be negligible
<b>Sensitivity coefficient</b>	<1	Assumed to be negligible
<b>Correlation(s) between affected parameters</b>	None	May be linked to the chosen backscattering Raman cross-section
<b>Element/step common for all sites/users?</b>	Yes	The different sites use different optical configurations to reduce the effects of spatial inhomogeneities of the detector photocatode
<b>Traceable to ...</b>	No	
<b>Validation</b>	[8,9]	

## 5.6 Acquisition (4)

A trigger circuit synchronizes the acquisition of the electric signal from the detector with the emission of each laser pulse in order to measure the intensity of the Raman backscattered light from the atmosphere at different distances from the transmitter. This is the Raman lidar signal. Usually, the acquisition of this signal is performed both in analog and photon counting mode, in order to increase the detectable dynamic range of lidar signals: for analog acquisition, an Analog to Digital Converter (ADC) is used to sample the average voltage produced by the incident photons on the detector, at regular time intervals  $\tau_d$  (time resolution or sampling time of the acquisition system) after the emission of each laser pulse; for photon counting acquisition, a counting system (a discriminator plus a fast counter) is used to measure the number of incident photons on the detector at regular time intervals  $\tau_d$  after the emission of each laser pulse. For both analog and photon counting Raman signals the vertical resolution, determined by the time resolution of the acquisition system, typically ranges from a few meters up to a few tens of meters.

The uncertainty contributions of the acquisition system are related to the background contribution  $P_B$  of lidar signals, the response time of the acquisition system in photon counting mode and any asynchrony between the emission of laser pulses and signal acquisition. These cause biases and distortions in both analog and photon counting Raman signals, which result in biases and distortions in the retrieved aerosol extinction coefficient profile. In EARLINET algorithms, lidar signals are corrected for all these effects in the pre-processing phase (see section 6), where the uncertainty and correlation effects of each contribution are described in the corresponding sub-level section. After these corrections, all the contributions of the acquisition system to the uncertainty of aerosol extinction coefficient profile are assumed negligible.

Information / data	Type / value / equation	Notes / description
<b>Name of effect</b>	Acquisition	Contribution related to conversion of the electric signal from the detector to a lidar signal (both in analog and photon counting mode)
<b>Contribution identifier</b>	4	
<b>Measurement equation parameter(s) subject to effect</b>	$P_B$ and $z$ in lidar equation of Raman signals at $\lambda_S = 607nm$	

<b>Contribution subject to effect (final product or sub-tree intermediate product)</b>	Aerosol extinction coefficient profile $\alpha(z)$	
<b>Time correlation extent &amp; form</b>	See sub-levels 6a,6b,6c,6d	
<b>Other (non-time) correlation extent &amp; form</b>	See sub-levels 6a,6b,6c,6d	
<b>Uncertainty PDF shape</b>	N/A	Systematic effect
<b>Uncertainty &amp; units</b>	0% (relative uncertainty) combination of 6a,6b,6c,6d	Assumed to be negligible
<b>Sensitivity coefficient</b>	1	
<b>Correlation(s) between affected parameters</b>	See sub-levels 6a,6b,6c,6d	
<b>Element/step common for all sites/users?</b>	Yes	
<b>Traceable to ...</b>	See sub-levels 6a,6b,6c,6d	
<b>Validation</b>	See sub-levels 6a,6b,6c,6d	

## 5.7 Raw Raman signals (5)

Both analog and photon counting Raman signals produced by single laser pulses are integrated over a fixed time interval, that is over a fixed number of laser shots, depending on the pulse repetition rate of the lidar. This is done for two main reasons: firstly, the lidar technique is commonly used to study atmospheric processes with a dynamic which is usually much slower than the time characteristic of the single shot lidar profiles; secondly, the electronic setup allowing to store single shot lidar profiles is quite demanding. Typically, the raw lidar signals used in EARLINET algorithms have a time resolution ranging from 10 to 60 s and a vertical resolution from a few meters up to a few tens of meters.

Raw Raman signals are provided with their random uncertainty, which is the standard deviation of the Poisson distribution of counts (square root of the counts) for photon counting signals. For analog signals the random uncertainty, which is the standard deviation of the normal distribution of voltages is usually not provided. The random uncertainty of raw Raman signals produces a random uncertainty in the aerosol extinction profile, depending on the following processing of raw Raman signals, which in turn depends on aerosol load and specifications of each instrument. As raw Raman signals are not directly used in the retrieval algorithm of aerosol extinction profile, the random uncertainty that they produce in such direct retrieval is not provided.

Information / data	Type / value / equation	Notes / description
<b>Name of effect</b>	Raw Raman signals	Contribution of random uncertainty of raw Raman signals
<b>Contribution identifier</b>	5	
<b>Measurement equation parameter(s) subject to effect</b>	Lidar equation of Raman signals at $\lambda_s = 607nm$	

<b>Contribution subject to effect (final product or sub-tree intermediate product)</b>	Aerosol extinction coefficient profile $\alpha(z)$	
<b>Time correlation extent &amp; form</b>	N/A	
<b>Other (non-time) correlation extent &amp; form</b>	N/A	
<b>Uncertainty PDF shape</b>	Poisson/normal distribution for photon counting/analog signals;	Statistical uncertainty
<b>Uncertainty &amp; units</b>	N/A	Depending on the following processing of raw Raman signals.
<b>Sensitivity coefficient</b>	1	
<b>Correlation(s) between affected parameters</b>	N/A	
<b>Element/step common for all sites/users?</b>	Yes	Changes according to the system experimental setup
<b>Traceable to ...</b>	N/A	
<b>Validation</b>	No	

## 5.8 Pre-processing of Raman signals (6)

The raw Raman signals are pre-processed to apply instrumental corrections and, optionally, a vertical smoothing or temporal averaging. This stage is commonly known as “pre-processing” of lidar signals and represents a necessary step to apply the aerosol extinction profile retrieval algorithm. The pre-processing procedure contains the following steps: dead time correction (6a), dark subtraction (6b), trigger delay/first range bin correction (6c), background subtraction (6d), vertical integration or binning (6e), temporal integration (6f), signal gluing (6g) and overlap correction (6h).

The pre-processed Raman signals have time and vertical resolutions depending, respectively, on temporal and vertical integration performed by the pre-processing module. Typically, time and vertical resolutions range from a few tens of minutes to a few hours and from 30 to 60 m, respectively. The uncertainty residual contributions in aerosol extinction profile due to systematic effects are assumed negligible due to the instrumental corrections (6a, 6b, 6c, 6d, 6h) applied to the signals.

The random or statistical uncertainties of raw Raman signals are propagated at each step of the pre-processing, from the beginning to the end of the pre-processing chain, using the standard formula of statistical uncertainty propagation. For example, for the lidar station of Potenza, Italy, the random uncertainty of the pre-processed Raman signals is typically less than 10% through the entire troposphere and possibly higher, between 10% and 20%, in the vertical range from 10 to 12 km, with a vertical resolution of 60 m and a time resolution between 1 and 2 hours.

The resulting random uncertainty of the pre-processed Raman signals produces a random uncertainty in the aerosol extinction profile. As this random uncertainty depends on the following processing applied on the pre-processed signals, it is not provided at this step.

The uncertainty contribution to the aerosol extinction profile due to the pre-processing is the combination of contributions of several steps, whose uncertainties and correlations are described in the corresponding sub-level sections.

Information / data	Type / value / equation	Notes / description
<b>Name of effect</b>	Pre-processing	Combined contribution of all the pre-processing steps 6a, 6b, ... 6h applied to the raw signals
<b>Contribution identifier</b>	6	
<b>Measurement equation parameter(s) subject to effect</b>	Lidar equation of Raman signals at $\lambda_s = 607nm$	
<b>Contribution subject to effect (final product or sub-tree intermediate product)</b>	Aerosol extinction coefficient profile $\alpha(z)$	
<b>Time correlation extent &amp; form</b>	Different correlation scales	See inside the different pre-processing steps
<b>Other (non-time) correlation extent &amp; form</b>	Different correlation scales	See inside the different pre-processing steps
<b>Uncertainty PDF shape</b>	Poisson/normal distribution for photon counting/analog signals	Statistical uncertainty
<b>Uncertainty &amp; units</b>	N/A combination of 6a,6b,6c,6d, 6e, 6f, 6g, 6h	Depending on the following processing of pre-processed Raman signals.
<b>Sensitivity coefficient</b>	1	
<b>Correlation(s) between affected parameters</b>	N/A	
<b>Element/step common for all sites/users?</b>	Yes	Changes according to the system experimental setup.
<b>Traceable to ...</b>	N/A	
<b>Validation</b>	See inside the different pre-processing steps	

## 5.9 Dead Time correction (6a)

Each acquisition system in photon counting mode is characterized by a dead time, or response time, a time interval during which the system is unable to count incident photons. As a result, the acquisition is characterized by a maximum count rate above which the observed count rate is no longer proportional to the number of incident photons, but depends instead on the dead time duration. Therefore, for high count rates, typically occurring in the near range, raw Raman signals in photon counting mode are affected by distortions which result in artifacts in the retrieved aerosol extinction coefficient profile. These signals can be corrected using two different ideal models describing a photon counting system: a paralyzable model and a not paralyzable one. A paralyzable system is unable to record a second output pulse unless there is a time interval of at least the dead time  $\tau$  between two successive input pulses. If an additional pulse arrives during the response time, the dead time of the system is further extended by  $\tau$ . For high count rates, the system is not able to respond and it remains completely paralyzed, by providing a zero count rate. By using Poisson probability distribution, a paralyzable system is described by the following formula [10]:

$$N_m = N_r \exp(-\tau N_r)$$

where  $N_m$  and  $N_r$  are the measured count rate and the real count rate, respectively. In a not paralyzable system the dead time  $\tau$  is independent of the arrival of additional counts. For high count rates, the system will asymptotically approach a maximum count rate,  $N_{max}$ , which is the inverse of the dead time. A not paralyzable system is described by the following formula [10]:

$$N_m = \frac{N_r}{1 + \tau N_r}$$

The correction for dead time is performed by inverting one of the two previous equations with respect to the real count rate  $N_r$ , given the known value of dead time. Concerning the equation to be used, it is necessary to specify that real systems are never completely paralyzable or not paralyzable, but their behavior is somewhat intermediate between these two ideal models. Therefore, neither of the two previous equations describes a real photon counting system accurately. However, for count rates not too high, typically  $< 10\text{--}30$  MHz depending on the value of  $\tau$ , the two models produce very similar results and the choice between the two models becomes irrelevant [2]. The dead time value can be accurately measured as described in Johnson et al. [11, 12] or is provided by the PMT manufacturer. In EARLINET algorithms, the raw Raman signals in photon counting mode are always corrected for dead time (wherever it is possible) and particular care is addressed to the optimization of lidar channel in order to not have too high count rates. Under these conditions, the uncertainty of aerosol extinction coefficient profile due to the dead time correction is assumed negligible.

Information / data	Type / value / equation	Notes / description
<b>Name of effect</b>	Dead time correction	Contribution due to the response time of photon counting acquisition system
<b>Contribution identifier</b>	6a	
<b>Measurement equation parameter(s) subject to effect</b>	Lidar equation of raw Raman signals at $\lambda_s = 607nm$ in photon counting mode	
<b>Contribution subject to effect (final product or sub-tree intermediate product)</b>	Aerosol extinction coefficient profile $\alpha(z)$	
<b>Time correlation extent &amp; form</b>	Possible long term correlation (the dead time is not necessarily constant and should be measured regularly)	Extent & form not quantified
<b>Other (non-time) correlation extent &amp; form</b>	Correlation with vertical range because only the lower part of extinction profile is affected	Extent & form not quantified
<b>Uncertainty PDF shape</b>	N/A	Systematic effect
<b>Uncertainty &amp; units</b>	0% (relative uncertainty)	Assumed to be negligible (the dead time measured or provided by the manufacturer)

		as well as correction formula are very accurate)
<b>Sensitivity coefficient</b>	1	
<b>Correlation(s) between affected parameters</b>	N/A	
<b>Element/step common for all sites/users?</b>	Yes	Two different correction models are applied: paralyzable and non-paralyzable
<b>Traceable to ...</b>	No	Manufacturer specifications or measurements performed at each lidar station
<b>Validation</b>	[2 ,10, 11, 12]	

### 5.10 Dark subtraction (6b)

Raw Raman signals acquired in analog mode can be affected by electronic distortions not related to the Raman backscattered light from the atmosphere and mainly caused by the laser power circuits, the detector dark current (temperature dependent) and the amplification circuits of the analog acquisition system. These electronic distortions result in distortions in the aerosol extinction coefficient profile, which depend on both the lidar system and the particular measurement session. Analog raw Raman signals are corrected for electronic distortions by performing the dark subtraction, typically consisting in the following procedure:

- 1) N raw signals are acquired with the telescope completely obstructed, before or after the acquisition of the ordinary raw signals of each measurement session. These dark signals are not affected by any light backscattered from the atmosphere and may contain only the electronic distortions.
- 2) The N dark signals are averaged for each range bin; the random uncertainty of the average dark signal can also be calculated as the standard deviation of the dark signals (voltages) for each range bin.
- 3) From each raw Raman signal the average dark signal obtained in the previous step is subtracted to obtain the raw Raman signal corrected for electronic distortions. The random uncertainty of this signal can be calculated by combining in quadrature the uncertainties of the uncorrected raw Raman signal and of the average dark signal.

In EARLINET algorithms, where raw Raman signals in analog mode are dark subtracted, the residual contribution to the uncertainty of aerosol extinction coefficient profile due to electronic distortions is assumed negligible, assuming that electronic distortions remain stable in the time interval between dark and ordinary signals acquisition.

Information / data	Type / value / equation	Notes / description
<b>Name of effect</b>	Dark subtraction	Contribution of electronic distortions in analog signals
<b>Contribution identifier</b>	6b	

<b>Measurement equation parameter(s) subject to effect</b>	$P_B$ in lidar equation of raw Raman signals at $\lambda_S = 607nm$ in analog mode	
<b>Contribution subject to effect (final product or sub-tree intermediate product)</b>	Aerosol extinction coefficient profile $\alpha(z)$	
<b>Time correlation extent &amp; form</b>	Various time scales	Extent & form not quantified (dark signals are acquired for each measurement session)
<b>Other (non-time) correlation extent &amp; form</b>	Possible correlation with the temperature of detector	Extent & form not quantified
<b>Uncertainty PDF shape</b>	N/A	Systematic effect
<b>Uncertainty &amp; units</b>	0% (relative uncertainty)	Assumed to be negligible due to dark subtraction from analog raw Raman signals
<b>Sensitivity coefficient</b>	1	
<b>Correlation(s) between affected parameters</b>	N/A	
<b>Element/step common for all sites/users?</b>	Yes	The number of dark signals and their averaging time can change for the different stations
<b>Traceable to ...</b>	N/A	
<b>Validation</b>	No	

### 5.11 First range bin/Trigger delay (6c)

The electronics of both the acquisition system and the trigger, which provides the logic signals for the start of the acquisition, can cause a discrepancy between the instant of emission of a laser pulse and the start of the acquisition related to that laser pulse. Two different situations may occur. In the first, the start of the acquisition is delayed compared to the instant of emission of the laser pulse and the discrepancy  $dt$ , called *trigger delay*, results in an underestimation  $dz$  of the altitudes in Raman signals. Alternatively, the start of the acquisition is in advance compared to the instant of emission of the laser pulse and the discrepancy  $dt$ , called *first range bin*, results in an overestimation  $dz$  of the altitudes in Raman signals. The above discrepancy, trigger delay or first range bin, affects both analog and photon counting acquisition, is generally different for each channel and leads to errors not only in the determination of the altitudes in Raman signals, but also in the retrieval of aerosol extinction coefficient profile, especially in the near range.

The measurement of trigger delay or first range bin and the calculus of absolute error in aerosol extinction coefficient profile due to this discrepancy are described in [7,13]. Raw Raman signals both in analog and photon counting mode are corrected by interpolating them to the correct time or range bins [2]. Consider, for example, a lidar channel with vertical resolution of 15m, corresponding to a dwell time of 100ns. Suppose also that the same channel is affected by a trigger delay/first range bin of  $dt$ . The raw uncorrected lidar signal of the channel is  $S_{raw}=\{(t_1,s_1), (t_2,s_2), \dots (t_n,s_n)\}$ , where the instants  $t_i$  are 50, 150, 250, ... ns, corresponding, in the range domain, to 7.5, 22.5, 37.5, ... m. Because the channel is affected by a trigger delay/first range bin of  $dt$ , the measured intensities  $s_1, s_2, \dots s_n$  refer to the instants  $t_1+dt, t_2+dt, \dots t_n+dt$  and not to the instants  $t_1, t_2, \dots t_n$ . As a consequence, the correct

association between measured intensities and times-range bins should be  $S_{corr}=\{(t_1+dt,s_1), (t_2+dt,s_2), \dots, (t_n+dt,s_n)\}$ .

In EARLINET algorithms, where raw Raman signals are corrected for trigger delay/first range bin, the residual contribution to the uncertainty of aerosol extinction coefficient profile due to the trigger delay/first range bin correction is assumed negligible.

Information / data	Type / value / equation	Notes / description
<b>Name of effect</b>	First range bin/Trigger delay correction	Contribution due to asynchrony between the emission of laser pulses and the start of signal acquisition in both analog and photon counting channels
<b>Contribution identifier</b>	6c	
<b>Measurement equation parameter(s) subject to effect</b>	Altitude $z$ in lidar equation of raw Raman signals at $\lambda_S = 607nm$ in both analog and photon counting mode	
<b>Contribution subject to effect (final product or sub-tree intermediate product)</b>	Aerosol extinction coefficient profile $\alpha(z)$	
<b>Time correlation extent &amp; form</b>	Possible long term correlation due to long term instability of trigger delay/first range bin	Extent & form not quantified
<b>Other (non-time) correlation extent &amp; form</b>	1) Correlation with vertical range: the lower part of extinction profile is mostly affected; 2) Possible correlation with vertical range if the value of trigger delay/first range bin is not a multiple of the time resolution of the acquisition system	1) Extent & form quantified in [7] 2) Extent & form not quantified
<b>Uncertainty PDF shape</b>	N/A	Systematic effect
<b>Uncertainty &amp; units</b>	0% (relative uncertainty)	Assumed to be negligible due to the first range bin/trigger delay correction of raw Raman signals
<b>Sensitivity coefficient</b>	1	
<b>Correlation(s) between affected parameters</b>	N/A	
<b>Element/step common for all sites/users?</b>	Yes	Measurement techniques and values of trigger delay/first range bin can change for the different lidar stations
<b>Traceable to ...</b>	No	Trigger delay/first range bin measurements performed at

		each lidar station with accuracy within the time resolution of the acquisition system
<b>Validation</b>	[2, 7, 13]	

### 5.12 Background subtraction (6d)

Raw Raman signals measured both in analog and photon counting mode consist of two contributions: the contribution of Raman backscattered light from the atmosphere and the background contribution, generated by direct or scattered sunlight in day time, or by the moon, stars and artificial light sources at night time. The background signal, range independent, is an uncertainty source for Raman signals and, consequently, for the retrieved aerosol extinction coefficient profile. Therefore, it is necessary to subtract from each raw Raman signal its background contribution, in order to consider only the signal due to the Raman backscattered light from the atmosphere. Because this signal decreases with increasing range, the background contribution of a raw Raman signal is usually obtained by averaging it in the far range, above 20km, where the signal due to the backscattering from the atmosphere is neglectable with respect to the background signal. The random uncertainty of the background signal is calculated as the standard deviation of the values of the raw Raman signal within the selected averaging range in the far range [14].

From each raw Raman signal, both in analog and photon counting mode, the corresponding background signal is subtracted. The random uncertainty of this background subtracted raw Raman signal is calculated by combining in quadrature the uncertainties of the raw Raman signal and of the background signal [14].

Note that for an ideal lidar system the background signal includes also the range independent dark contribution which, therefore, should not be subtracted from the raw analog signals. However, in real systems, with range dependent electronic distortions in analog raw signals, the dark signal needs to be separately subtracted from analog raw signals in order to remove these distortions.

In EARLINET algorithms, where raw Raman signals, both in analog and photon counting mode, are background subtracted, the residual contribution to the uncertainty of aerosol extinction coefficient profile due to the background signals is assumed negligible.

Information / data	Type / value / equation	Notes / description
<b>Name of effect</b>	Background subtraction	Contribution of background in analog and photon counting signals
<b>Contribution identifier</b>	6d	
<b>Measurement equation parameter(s) subject to effect</b>	$P_B$ in lidar equation of raw Raman signals at $\lambda_S = 607nm$ in both analog and photon counting mode	
<b>Contribution subject to effect (final product or sub-tree intermediate product)</b>	Aerosol extinction coefficient profile $\alpha(z)$	

<b>Time correlation extent &amp; form</b>	Possible correlation with the time of measurement session	Extent & form not quantified
<b>Other (non-time) correlation extent &amp; form</b>	Possible correlation with background light, bandwidth of 607nm interference filter and field of view of the receiver	Extent & form not quantified
<b>Uncertainty PDF shape</b>	N/A	Systematic effect
<b>Uncertainty &amp; units</b>	0% (relative uncertainty)	Assumed to be negligible due to background subtraction from raw Raman signals
<b>Sensitivity coefficient</b>	1	
<b>Correlation(s) between affected parameters</b>	N/A	
<b>Element/step common for all sites/users?</b>	Yes	
<b>Traceable to ...</b>	N/A	
<b>Validation</b>	[14]	

### 5.13 Vertical integration (binning) (6e)

Raw Raman signals are usually vertically integrated or smoothed (binning), in order to increase their signal to noise ratio (SNR) or, equivalently, to reduce their relative random uncertainty. In binned signals each point is obtained by summing (photon counting) or averaging (analog) the acquired signals (counts or voltages) in a certain number of range bins and associating as height the mean of the height range relative to the binned range points. The random uncertainty of each point is then calculated by combining in quadrature the random uncertainties (standard deviations) of signals in the binned ranges [14]. The binning reduces the vertical resolution of raw Raman signals to values typically ranging from 30 to 60m. The random uncertainty of the binned raw Raman signals produces a random uncertainty in the aerosol extinction profile which depends on the following processing of these signals. As binned raw Raman signals are not directly used in the retrieval algorithm of aerosol extinction profile, the random uncertainty that they produce in such direct retrieval is not provided.

Information / data	Type / value / equation	Notes / description
<b>Name of effect</b>	Vertical integration (binning)	Contribution of vertical integration of raw Raman signals
<b>Contribution identifier</b>	6e	
<b>Measurement equation parameter(s) subject to effect</b>	Lidar equation of Raman signals at $\lambda_S = 607nm$	
<b>Contribution subject to effect (final product or sub-tree intermediate product)</b>	Aerosol extinction coefficient profile $\alpha(z)$	
<b>Time correlation extent &amp; form</b>	N/A	

<b>Other (non-time) correlation extent &amp; form</b>	Possible correlation with the binning range (i.e. the number of range bins)	Extent & form not quantified
<b>Uncertainty PDF shape</b>	Poisson/normal distribution for photon counting/analog signals;	Statistical uncertainty
<b>Uncertainty &amp; units</b>	N/A	Depending on the following processing of binned raw Raman signals.
<b>Sensitivity coefficient</b>	1	
<b>Correlation(s) between affected parameters</b>	N/A	
<b>Element/step common for all sites/users?</b>	Yes	The number of binned points, the vertical resolution and random uncertainty of binned raw Raman signals can change for the different stations
<b>Traceable to ...</b>	N/A	
<b>Validation</b>	[14]	

#### 5.14 Temporal integration (6f)

In order to further increase their SNR, binned raw Raman signals are temporally integrated, by summing (photon counting) or averaging (analog) them over a time interval from a few tens of minutes to a few hours, depending on the observed atmospheric scenario. The random uncertainty of the resulting time integrated signals is obtained, for each range bin, by combining in quadrature the random uncertainties (standard deviations) of single signals that are integrated. The uncertainty of time integrated Raman signals affects the random uncertainty of the aerosol extinction profile which depends on the following processing of these signals. The integration time of raw Raman signals is carefully selected so that during this time the atmosphere is stable and the uncertainty contribution to the aerosol extinction profile due to the atmospheric variability can be considered negligible.

As time integrated Raman signals are not directly used in the retrieval algorithm of aerosol extinction profiles, the random uncertainty that they produce in such direct retrieval is not provided.

Information / data	Type / value / equation	Notes / description
<b>Name of effect</b>	Temporal integration	Contribution of temporal integration of raw Raman signals
<b>Contribution identifier</b>	6f	
<b>Measurement equation parameter(s) subject to effect</b>	Lidar equation of Raman signals at $\lambda_s = 607nm$	
<b>Contribution subject to effect (final product or sub-tree intermediate product)</b>	Aerosol extinction coefficient profile $\alpha(z)$	
<b>Time correlation extent &amp; form</b>	Various time scales	Extent & form not quantified (the integration time changes)

		for each measurement session)
<b>Other (non-time) correlation extent &amp; form</b>	N/A	
<b>Uncertainty PDF shape</b>	Poisson/normal distribution for photon counting/analog signals	Statistical uncertainty
<b>Uncertainty &amp; units</b>	N/A	Depending on the following processing of time integrated Raman signals.
<b>Sensitivity coefficient</b>	1	
<b>Correlation(s) between affected parameters</b>	N/A	
<b>Element/step common for all sites/users?</b>	Yes	The integration time and random uncertainty of time integrated Raman signals can change for the different stations according to the system experimental setup.
<b>Traceable to ...</b>	N/A	
<b>Validation</b>	No	

### 5.15 Signal gluing (6g)

The dynamic range of tropospheric lidar signals is very high (at least 4 orders of magnitude). In the near range the signal is extremely high, while in the far range it is extremely weak. In both of these extreme conditions, a good signal to noise ratio and linearity between light intensity and measured signal are required. Lidar signals acquired in analog mode have a high signal to noise ratio in the near range, but a low signal to noise ratio and possible distortions in the far range. On the other hand, lidar signals acquired in photon counting mode show a very good signal to noise ratio in the far range, but they are problematic for high count rates, that occurs in the near range. In these conditions, the signals in photon counting mode lose their linearity due to the dead time and the greater the count rate, the more difficult it is to correct for this effect. Given the complementarity between analog and photon counting signals, it is possible to extend the detectable dynamic range of lidar, by appropriately combining the analog and photon counting signals resulting from the previous pre-processing steps. In particular, it is assumed that the “main” signal is the signal in photon counting mode and the corresponding analog signal is considered just an extension of the signal in photon counting mode in the near range. Generally, this operation is called gluing between analog and photon counting signals. This gluing is usually performed by the following steps [2]:

- 1) Identifying a minimum range  $z_{\min}$  above which non linear effects in the photon counting signal, due to the dead time, are absent or corrected in reliable way. Typically,  $z_{\min}$  corresponds to a count rate of about 10-30MHz in the photon counting signal [15, 16, 17]
- 2) Identifying a maximum range  $z_{\max}$  below which distorsions in the analog signal are neglectable. This maximum range corresponds to a value of the analog signal of  $V_{fs}/K$ , where  $V_{fs}$  is the maximum acquisition value and  $K$  is a factor depending on the quality of the ADC. (Typically  $K$  ranges from 5000 to 20000).

- 3)  $z_{max}$  and  $z_{min}$  are selected so that  $z_{max}$  is higher than  $z_{min}$  and analog and photon counting signals can be glued; if this is not possible, the gluing is not performed and the following processing steps are generally applied only to the photon counting signal above  $z_{min}$ .
- 4) A linear fit of photon counting signal and of analog signal is performed in the interval  $[z_{min}, z_{max} - dz]$ , with  $dz = 0$ .
- 5) If the coefficients of linear fits in the previous step are consistent, the procedure goes to the next step; otherwise, it returns to the step 4) with  $dz = z$ , where  $z$  is a multiple of the vertical resolution of lidar signals resulting from the previous pre-processing steps (typically ranging from 30 to 60m).
- 6) The analog signal is scaled on the photon counting signal by a linear fit in the interval  $[z_{min}, z_{max} - dz]$ . The gluing factor  $a$  is calculated by minimizing the following quantity:

$$\sum_i [S_{PC}(z_i) - aS_{analog}(z_i)]^2$$

where  $S_{PC}$  and  $S_{analog}$  are photon counting and analog signals resulting from the previous pre-processing steps in the gluing range.

- 7) The gluing point is identified in the interval  $[z_{min}, z_{max} - dz]$  as the point for which the squared difference between the analog signal and photon counting signal is minimum.
- 8) Finally, the glued signal is formed by the scaled analog signal, for ranges below the gluing point, and by the photon counting signal for ranges above the gluing point.

The random uncertainty of the glued signal is the random uncertainty of the scaled analog signal (obtained by uncertainty propagation formula) and of photon counting signal, respectively below and above the gluing point. This uncertainty produces the random uncertainty of the aerosol extinction profile. As this random uncertainty depends on the following processing of glued Raman signals, it is not provided at this step.

Information / data	Type / value / equation	Notes / description
<b>Name of effect</b>	Signal gluing	Contribution due to the combination of analog and photon counting signals
<b>Contribution identifier</b>	6g	
<b>Measurement equation parameter(s) subject to effect</b>	Lidar equation of Raman signals at $\lambda_s = 607nm$	
<b>Contribution subject to effect (final product or sub-tree intermediate product)</b>	Aerosol extinction coefficient profile $\alpha(z)$	
<b>Time correlation extent &amp; form</b>	N/A	
<b>Other (non-time) correlation extent &amp; form</b>	Possible correlation with the gluing range	Extent & form not quantified
<b>Uncertainty PDF shape</b>	Normal/Poisson distribution below/above the gluing point	Statistical uncertainty
<b>Uncertainty &amp; units</b>	N/A	Depending on the following processing of glued Raman signals

<b>Sensitivity coefficient</b>	1	
<b>Correlation(s) between affected parameters</b>	N/A	
<b>Element/step common for all sites/users?</b>	Yes	Similar methods for the different stations
<b>Traceable to ...</b>	N/A	
<b>Validation</b>	[2, 15, 16, 17]	

## 5.16 Overlap Correction (6h)

The glued Raman signal, resulting from the previous pre-processing steps, can be corrected for incomplete overlap by using a suitable overlap function, depending on the lidar geometry, that is the combination of all geometric factors, including the laser beam diameter, shape, divergence and tilt, the telescope focal ratio, the receiver field of view and the location of emitter and receiver optical axes relative to each other (coaxial or biaxial configuration). The overlap function  $O(z)$  and the full overlap height  $z_{ovl}$  can be determined both theoretically and experimentally. Theoretical determination can be performed by raytracing simulations or by the methods described in Kuze et al. [18], Measures [19], and Chourdakis et al. [20]. Experimental determination can be performed by measurements at different zenith angles under homogeneous and stationary atmospheric conditions, or by the methods described in Wandinger and Ansmann [21] and Freudenthaler [22].

If the Raman signal is not corrected with an overlap function, the resulting uncertainty in the aerosol extinction profile at heights below  $z_{ovl}$  can reach 50% [21]; in this case, the provided extinction profile is cut below  $z_{ovl}$ , typically ranging from 250 to 500 m above the ground, depending on the lidar system, and above  $z_{ovl}$  the systematic uncertainty in the extinction profile due to the overlap function is assumed negligible.

If the Raman signal is corrected for overlap, the extinction profile is provided starting from a minimum height  $z_0 < z_{ovl}$  above which the profile is considered trustworthy and the residual uncertainty due to the overlap function is assumed negligible. In EARLINET stations, lidar signals are usually not corrected for overlap and extinction profiles are provided starting from  $z_{ovl}$ .

Information / data	Type / value / equation	Notes / description
<b>Name of effect</b>	Overlap correction	Contribution due to the correction with overlap function
<b>Contribution identifier</b>	6h	
<b>Measurement equation parameter(s) subject to effect</b>	$O(z)$ in lidar equation of Raman signals at $\lambda_S = 607nm$	
<b>Contribution subject to effect (final product or sub-tree intermediate product)</b>	Aerosol extinction coefficient profile $\alpha(z)$	
<b>Time correlation extent &amp; form</b>	Possible long term correlation ( $O(z)$ is not necessarily constant and should be determined regularly)	Extent & form not quantified
<b>Other (non-time) correlation extent &amp; form</b>	Correlation with vertical range (only the lower part of extinction profile from ground to $z_{ovl}/z_0$ is affected)	Extent & form not quantified
<b>Uncertainty PDF shape</b>	N/A	Systematic effect

<b>Uncertainty &amp; units</b>	0% for $z > z_{ovl}/z_0$ up to 50% for $z < z_{ovl}/z_0$	Assumed to be negligible due to the cut of the extinction profile below $z_{ovl}$ or $z_0 < z_{ovl}$
<b>Sensitivity coefficient</b>	1	
<b>Correlation(s) between affected parameters</b>	N/A	
<b>Element/step common for all sites/users?</b>	Yes	Usually, overlap correction is not applied in EARLINET lidar stations
<b>Traceable to ...</b>	N/A	
<b>Validation</b>	[18, 19, 20, 21, 22]	

### 5.17 Processing of Raman signals (7)

The processing of Raman signals to retrieve the aerosol extinction coefficient profile comprises several steps. First, an estimation of molecular density profile and the corresponding molecular extinction profile (7a) is needed. In particular, the atmospheric nitrogen number density profile and the molecular extinction coefficient profiles at wavelengths  $\lambda_L$  and  $\lambda_S$  are required. Secondly, an assumption of aerosol Ångström exponent (7b) and, optionally, the correction for multiple scattering (7c) are required. Finally, suitable and stable numerical methods are needed to calculate the derivative present in the equation (3) for the retrieval of aerosol extinction coefficient profile.

The profile of aerosol extinction coefficient has a time sampling which is the integration time used in pre-processing of Raman signals, ranging from a few tens of minutes to a few hours. The effective vertical resolution of aerosol extinction profile ranges from a few hundreds of meters to many hundreds of meters, depending on the vertical integration (binning) performed in pre-processing of Raman signals and on method and vertical smoothing used to calculate the derivative in equation (3) [25].

The uncertainty contributions for the retrieval of aerosol extinction profile are systematic, associated to assumptions and corrections described above, and statistical, due to the propagation of random uncertainty of pre-processed Raman signal.

Total maximum systematic uncertainty, calculated by combining all systematic contributions less than 10% (7a, 7b, 7c), is less than 15% for extinction coefficient values higher than  $2 \times 10^{-5} \text{ m}^{-1}$  and greater for lower extinction coefficient values. On the other hand, random uncertainty estimates are typically less than 10% for extinction coefficient values higher than  $2 \times 10^{-5} \text{ m}^{-1}$  and greater for lower extinction coefficient values (7d).

The total uncertainty of aerosol extinction profile due to the processing is the combination of contributions of each step, whose uncertainties and correlation effects are described in the corresponding sub-level sections.

Information / data	Type / value / equation	Notes / description
<b>Name of effect</b>	Processing of Raman signals	Combined contribution of all the processing steps 7a,7b,7c, 7d applied to the pre-processed Raman signals

<b>Contribution identifier</b>	7	
<b>Measurement equation parameter(s) subject to effect</b>	Raman equation (3) for the retrieval of aerosol extinction coefficient profile	Include additional correction related to spectral dependence and multiple scattering as well as assumptions on molecular density and extinction coefficient profiles
<b>Contribution subject to effect (final product or sub-tree intermediate product)</b>	Aerosol extinction coefficient profile $\alpha(z)$	
<b>Time correlation extent &amp; form</b>	Different correlation scales	See inside the different processing steps
<b>Other (non-time) correlation extent &amp; form</b>	Different correlation scales	See inside the different processing steps
<b>Uncertainty PDF shape</b>	N/A	Combination of propagated random and estimated systematic uncertainties
<b>Uncertainty &amp; units</b>	<p>Random:</p> <p>&lt;10% (<math>1\sigma</math>) for <math>\alpha(z) &gt; 2 \times 10^{-5} \text{m}^{-1}</math></p> <p>&gt;10% (<math>1\sigma</math>) for <math>\alpha(z) &lt; 2 \times 10^{-5} \text{m}^{-1}</math></p> <p>Systematic:</p> <p>&lt; 15% for <math>\alpha(z) &gt; 2 \times 10^{-5} \text{m}^{-1}</math></p> <p>&gt; 15% for <math>\alpha(z) &lt; 2 \times 10^{-5} \text{m}^{-1}</math></p> <p>Combination of 7a, 7b, 7c, 7d</p>	Combination of propagated random and estimated systematic uncertainties
<b>Sensitivity coefficient</b>	1	
<b>Correlation(s) between affected parameters</b>	N/A	
<b>Element/step common for all sites/users?</b>	Yes	Possible changes according to the different processing procedures at different lidar stations
<b>Traceable to ...</b>	N/A	
<b>Validation</b>	See inside the different processing steps	

### 5.18 Molecular density and extinction profiles (7a)

The number density profile of atmospheric nitrogen molecules  $N(z)$  is calculated from air density profile, which is obtained from atmospheric pressure and temperature profiles. These can be obtained

by using standard atmospheric models, provided by climatological models or measured by co-located and simultaneous radio-soundings. In EARLINET algorithms, models are typically used as co-located and simultaneous radio-soundings are not available due to their high cost. The profiles of molecular extinction coefficient  $\alpha_{\lambda_L}^{\text{mol}}(z)$  and  $\alpha_{\lambda_S}^{\text{mol}}(z)$  are calculated by using the Rayleigh scattering theory [26,27], and air density profile obtained from atmospheric pressure and temperature profiles. The uncertainty contribution to the aerosol extinction profile due to the assumption on molecular scattering cross sections, considered constant with the vertical range, is assumed negligible. On the other hand, temperature and pressure profiles used for the retrieval of molecular density profile may differ from the real profiles and these differences are a source of uncertainty in the retrieval of aerosol extinction profile. In particular, the difference between the temperature gradient  $dT/dz = -6.5\text{K/km}$  assumed in standard temperature profiles and real temperature gradients results in the most significant uncertainty contribution in the aerosol extinction coefficient profile. This uncertainty contribution can be considerable in presence of strong temperature inversions, typically occurring in the lower troposphere. For example, it has been estimated that a temperature gradient of 13 K/km in the altitude range between 1.8 and 2 km can produce an uncertainty in the aerosol extinction coefficient at the same range higher than 30% [28]. However, the uncertainty due to differences between assumed and real temperature gradients decreases with increasing vertical smoothing window length, that usually increases with increasing the vertical range.

Sensitivity studies, based on temperature and pressure profiles measured with radio-soundings, show that, without strong temperature inversions, so that differences between assumed and real (measured) temperature gradients are not too large, the systematic uncertainty contribution associated to the assumption of temperature and pressure profiles is typically less than 10%, but can also increase up to 30% for values of extinction coefficient lower than  $2 \times 10^{-5} \text{ m}^{-1}$  [28,29].

Lower or negligible uncertainty contributions can be obtained by using pressure and temperature profiles measured with co-located and simultaneous radio-soundings, if available, or provided by NWP re-analysis. To this end, in the future the EARLINET network will also provide non-NRT products obtained by reprocessing the lidar measurements with these pressure and temperature profiles.

Information / data	Type / value / equation	Notes / description
<b>Name of effect</b>	Molecular density and extinction profile	Contributions due to the assumption of molecular density and extinction profiles
<b>Contribution identifier</b>	7a	
<b>Measurement equation parameter(s) subject to effect</b>	$N(z)$ , $\alpha_{\lambda_L}^{\text{mol}}(z)$ and $\alpha_{\lambda_S}^{\text{mol}}(z)$ in Raman equation (3) for the retrieval of aerosol extinction coefficient profile	
<b>Contribution subject to effect (final product or sub-tree intermediate product)</b>	Aerosol extinction coefficient profile $\alpha(z)$	
<b>Time correlation extent &amp; form</b>	Possible long term correlation across multiple measurement sessions	Extent & form not quantified

<b>Other (non-time) correlation extent &amp; form</b>	Possible correlation with vertical range due to different lengths of vertical smoothing window at different altitude ranges	Extent & form not quantified
<b>Uncertainty PDF shape</b>	N/A	Systematic effect
<b>Uncertainty &amp; units</b>	< 10% for $\alpha(z) > 2 \times 10^{-5} \text{ m}^{-1}$ between 10% and 30% for $\alpha(z) < 2 \times 10^{-5} \text{ m}^{-1}$	Without strong temperature inversions
<b>Sensitivity coefficient</b>	1	
<b>Correlation(s) between affected parameters</b>	N/A	
<b>Element/step common for all sites/users?</b>	Yes	Different methods may be applied for obtaining the molecular density profile
<b>Traceable to ...</b>	N/A	
<b>Validation</b>	[26,27,28,29]	

### 5.19 Angstrom exponent assumption (7b)

The Ångström exponent  $\mathring{a}$ , as defined in equation (4), is an unknown dimensionless quantity that needs to be estimated. Typical values are in the range from 0 to 2. Fixed values are generally used. For ice particles of cirrus clouds the value of  $\mathring{a} = 0$  is used, while for aerosols most lidar stations, such as Potenza, use the value of  $\mathring{a} = 1$ , other stations use the value of  $\mathring{a} = 1.5$  or variable user-defined values according to actual meteorological conditions. Alternatively, values measured with sun photometers or derived from multi-wavelength simultaneous measurements of extinction coefficient are used.

The assumed value of Ångström exponent may differ from its real value, depending on specific microphysical properties of aerosol particles. Therefore, the assumption of Ångström exponent is a source of systematic uncertainty in the retrieval of the aerosol extinction profile. Sensitivity studies of aerosol extinction profile to the Ångström exponent show that a variation of the assumed value of 0.5 or 1 causes deviations of aerosol extinction profile less than 5% [28,30]. These deviations can be considered as a reasonable estimate of the uncertainty contribution to the aerosol extinction profile due to the Angstrom exponent assumption.

Information / data	Type / value / equation	Notes / description
<b>Name of effect</b>	Ångström exponent assumption	Contributions due to the assumption of Angstrom exponent
<b>Contribution identifier</b>	7b	
<b>Measurement equation parameter(s) subject to effect</b>	Ångström exponent $\mathring{a}$ defined by equation (4): $\frac{\alpha_{\lambda_L}^{par}(z)}{\alpha_{\lambda_S}^{par}(z)} = \left(\frac{\lambda_S}{\lambda_L}\right)^{\mathring{a}}$	

<b>Contribution subject to effect (final product or sub-tree intermediate product)</b>	Aerosol extinction coefficient profile $\alpha(z)$	
<b>Time correlation extent &amp; form</b>	Possible long term correlation across multiple measurement sessions	Extent & form not quantified
<b>Other (non-time) correlation extent &amp; form</b>	N/A	
<b>Uncertainty PDF shape</b>	N/A	Systematic effect
<b>Uncertainty &amp; units</b>	<5% (relative uncertainty)	
<b>Sensitivity coefficient</b>	1	
<b>Correlation(s) between affected parameters</b>	N/A	
<b>Element/step common for all sites/users?</b>	Yes	Different methods may be applied to estimate the Ångström exponent
<b>Traceable to ...</b>	N/A	
<b>Validation</b>	[28, 30]	

## 5.20 Multiple scattering correction (7c)

When the lidar laser beam goes through an optically dense medium, such as fog or clouds, not only the singly backscattered photons, but also photons undergoing multiple scattering processes may remain in the lidar receiver field of view and are forwarded to the receiving system. Under these conditions, lidar equations (1) and (3), valid only in single scattering approximation, are not valid anymore. This affects the extinction coefficient retrieval. The major effect of multiple scattering is to make lidar signals higher and extinction coefficient lower than those measured in single scattering conditions. The extinction coefficient profile can be corrected for multiple scattering, by introducing in lidar equations correction factors [31]. These are estimated from multiple scattering models that calculate multiple scattering intensities for lidar returns, considering the scattering characteristics of the scattering medium and the lidar system specifications, that is the receiver field of view, the laser beam divergence and the distance between the laser transmitter and the scattering volume [32].

In EARLINET algorithms, the correction of the extinction coefficient profile for multiple scattering is not performed. The uncertainty contribution in extinction coefficient profile without correction for multiple scattering is negligible in cloud-free atmosphere, 12% and 4% at the base and top of cirrus clouds, 10% and less than 3% at the base and inside cumulus clouds [28].

Information / data	Type / value / equation	Notes / description
<b>Name of effect</b>	Multiple scattering correction	Contribution due to the multiple scattering
<b>Contribution identifier</b>	7c	
<b>Measurement equation parameter(s) subject to effect</b>	Lidar equations (1) and (3) for the retrieval of aerosol extinction coefficient profile	

<b>Contribution subject to effect (final product or sub-tree intermediate product)</b>	Aerosol extinction coefficient profile $\alpha(z)$	
<b>Time correlation extent &amp; form</b>	Possible long term correlation depending on change in both the applied correction method and lidar system	Extent & form not quantified
<b>Other (non-time) correlation extent &amp; form</b>	Possible correlation with vertical range	For clouds: uncertainty at the base is greater than at the top; for aerosols: extent & form not quantified
<b>Uncertainty PDF shape</b>	N/A	Systematic effect
<b>Uncertainty &amp; units</b>	0% (relative uncertainty)	Correction for multiple scattering is not performed; uncertainty contribution assumed to be negligible for aerosols
<b>Sensitivity coefficient</b>	1	
<b>Correlation(s) between affected parameters</b>	N/A	
<b>Element/step common for all sites/users?</b>	Yes	Different models or corrections may be applied at different lidar stations
<b>Traceable to ...</b>	N/A	
<b>Validation</b>	[28,31,32]	

## 5.21 Retrieval of aerosol extinction coefficient profile (7d)

The processing algorithm requires the calculation of the derivative with respect to the range of the logarithm of the ratio between the number density profile of atmospheric nitrogen molecules and the range corrected pre-processed Raman signal. There are several methods to calculate the derivative in a stable way.

The most common methods use linear fit or digital filters, such as Savitzky-Golay filter [33]. The result of the derivative fluctuates substantially with vertical range so that a vertical smoothing must be applied. This implies a reduction of vertical resolution and statistical uncertainty with respect to the pre-processed Raman signal. The wider the smoothing window, the lower the effective vertical resolution and the statistical uncertainty. The methods to determine the relation between the length of the smoothing window and the resulting effective vertical resolution are described in [24,25]. Usually, as the statistical uncertainty increases with increasing the vertical range, different smoothing window lengths, increasing with the vertical range, are used, resulting in effective vertical resolution that decreases with increasing the vertical range. The effective vertical resolution of aerosol extinction profiles at 532nm provided by EARLINET database ranges from a few hundreds of meters to many hundreds of meters.

The statistical uncertainty of the pre-processed Raman signal propagates through the processing algorithm, resulting in the statistical uncertainty of the aerosol extinction coefficient profile. This can be estimated numerically, with the Monte Carlo method, or analytically, by means of error propagation theory applied to equation (3).

The Monte Carlo method is based on the random generation of new lidar signals. Each range bin of these signals is considered as a sample element of a probability distribution with a mean value and standard deviation that corresponds to the value and uncertainty of the pre-processed signal. The probability distribution is assumed to be Normal for the analog signal and Poissonian for the photo counting signal. The extracted lidar signals are then processed with the same algorithm used for the pre-processed signal, to produce a set of solutions in addition to that obtained from the pre-processed signal. The standard deviation of these solutions is finally used as the statistical uncertainty profile of the aerosol extinction profile obtained from the original pre-processed signal.

The statistical uncertainty of the aerosol extinction coefficient profile depends on the method by which the derivative is calculated, the applied smoothing and the method used to estimate the uncertainty itself. For the retrieval of aerosol extinction coefficient at 532 nm, random uncertainty estimates are typically less than 10% for values higher than  $2 \times 10^{-5} \text{ m}^{-1}$  and greater for lower extinction coefficient values. This typical value of random uncertainty has been evaluated as the median value of random uncertainties of aerosol extinction coefficient values greater than  $2 \times 10^{-5} \text{ m}^{-1}$  on the whole EARLINET quality assured database, involving measurements of 28 stations over Europe since 2000. From the same database, the typical detection limit for aerosol extinction coefficient of  $1 \times 10^{-6} \text{ m}^{-1}$  has been estimated as the value below which 95% of the values have a random uncertainty higher than 100%.

Information / data	Type / value / equation	Notes / description
<b>Name of effect</b>	Retrieval of aerosol extinction coefficient profile	Contribution due to the propagation of statistical uncertainty through the processing algorithm
<b>Contribution identifier</b>	7d	
<b>Measurement equation parameter(s) subject to effect</b>	Power of the pre-processed Raman signal $P_{\lambda_S}(z)$ at wavelength $\lambda_S = 607\text{nm}$ in Raman equation (3) for the retrieval of aerosol extinction coefficient profile	
<b>Contribution subject to effect (final product or sub-tree intermediate product)</b>	Aerosol extinction coefficient profile $\alpha(z)$	
<b>Time correlation extent &amp; form</b>	N/A	
<b>Other (non-time) correlation extent &amp; form</b>	Correlation with vertical range due to the smoothing	Extent & form not quantified (Depending on the method to calculate the derivative, the applied vertical smoothing and the method to calculate uncertainty)
<b>Uncertainty PDF shape</b>	Normal/Poisson distribution below/above the gluing point	Statistical uncertainty
<b>Uncertainty &amp; units</b>	$< 10\%$ ( $1\sigma$ ) for $\alpha(z) > 2 \times 10^{-5} \text{ m}^{-1}$	Depends on the method to calculate

	> 10% (1 $\sigma$ ) for $\alpha(z) < 2 \times 10^{-5} \text{ m}^{-1}$ Detection limit: $\alpha(z) = 1 \times 10^{-6} \text{ m}^{-1}$	the derivative, the applied vertical smoothing and the method to calculate uncertainty. Typical values are provided
<b>Sensitivity coefficient</b>	1	
<b>Correlation(s) between affected parameters</b>	N/A	
<b>Element/step common for all sites/users?</b>	Yes	Different smoothing and methods to calculate derivative and uncertainty may be applied.
<b>Traceable to ...</b>	N/A	
<b>Validation</b>	[25,33]	Validation by means of test functions like step function and Gaussian profile.

## 6 Uncertainty Summary

Element identifier	Contribution name	Uncertainty contribution form	Typical value	Traceability level (L/M/H)	random, structured random, quasi-systematic or systematic?	Correlated to? (Use element identifier)
1	Transmission system	N/A	0 %	M	systematic	none
2a	Receiver optical parameters	N/A	0 %	M	systematic	none
2b	Alignment of the lidar system	N/A	0 %	M	systematic	none
2	Receiving system	N/A	0 % combination of 2a & 2b	M	systematic	2a & 2b
3	Detectors	N/A	0 %	M	systematic	none
4	Acquisition	N/A	0 % combination of 6a, 6b,6c & 6d	M	systematic	6a, 6b,6c & 6d
5	Raw Raman signals	Poiss/norm distribution	N/A	M	random	6b, 6d,6e, 6f,6g & 7d
6a	Dead time correction	N/A	0 %	M	systematic	4
6b	Dark subtraction	N/A	0 %	M	systematic	4

6c	First range bin/Trigger delay correction	N/A	0 %	M	systematic	4
6d	Background subtraction	N/A	0 %	M	systematic	4
6e	Vertical integration (binning)	Poiss/norm distribution	N/A	M	random	5, 6b, 6d, 6f,6g & 7d
6f	Temporal integration	Poiss/norm distribution	N/A	M	random	5, 6b, 6d, 6e, 6g & 7d
6g	Signal gluing	Poiss/norm distribution	N/A	M	random	5, 6b, 6d, 6e, 6f & 7d
6h	Overlap correction	N/A	0% for $z > z_{ovl}/z_0$ up to 50% for $z < z_{ovl}/z_0$  0 %	M	systematic	none
6	Pre-processing	Poiss/norm distribution	N/A combination of 6a, 6b,6c, 6d,6e, 6f, 6g, 6h	M	random	5, 6a, 6b, 6c, 6d, 6e, 6f, 6g, 6h & 7d
7a	Molecular density and extinction profile	equation (3) for the retrieval of aerosol extinction coefficient profile	$< 10\%$ for $\alpha(z) > 2 \times 10^{-5} \text{ m}^{-1}$ $> 10\%$ for $\alpha(z) < 2 \times 10^{-5} \text{ m}^{-1}$	M	systematic	none
7b	Ångström exponent assumption	equation (3) for the retrieval of aerosol extinction coefficient profile	$< 5\%$	M	systematic	none
7c	Multiple scattering correction	N/A	0 %	M	systematic	none
7d	Retrieval of aerosol extinction coefficient profile	Poiss/norm distribution	$< 10\% (1\sigma)$ for $\alpha(z) > 2 \times 10^{-5} \text{ m}^{-1}$ $> 10\% (1\sigma)$ for $\alpha(z) < 2 \times 10^{-5} \text{ m}^{-1}$	M	random	5, 6b, 6d, 6e, 6f & 6g
7	Processing of Raman signals	N/A	Random: $< 10\% (1\sigma)$ for $\alpha(z) > 2 \times 10^{-5} \text{ m}^{-1}$	M	Random and systematic	5, 6b, 6d, 6e, 6f, 6g, 7a, 7b,7c, 7d

			<p>&gt;10%(1<math>\sigma</math>) for <math>\alpha(z) &lt; 2 \times 10^{-5} \text{m}^{-1}</math></p> <p>Systematic:</p> <p>&lt; 15% for <math>\alpha(z) &gt; 2 \times 10^{-5} \text{m}^{-1}</math></p> <p>&gt; 15% for <math>\alpha(z) &lt; 2 \times 10^{-5} \text{m}^{-1}</math></p> <p>combination of 7a, 7b,7c, 7d</p>			
--	--	--	--	--	--	--

Summarizing, the contributions of the main sources of uncertainty are as follows:

- Total statistical uncertainty  $U_{\text{stat}}$ , calculated starting from random uncertainties of raw lidar signals, by using the uncertainty propagation rules or Monte Carlo simulation for all applied signal handling procedures both in pre-processing and processing stages: dark subtraction, background subtraction, binning, temporal integration, signal gluing and the calculus of aerosol extinction coefficient  $\alpha(z)$  by equation (3), including a vertical smoothing.  
 $U_{\text{stat}}$  : < 10% for  $\alpha(z) > 2 \times 10^{-5} \text{m}^{-1}$ ; > 10% for  $\alpha(z) < 2 \times 10^{-5} \text{m}^{-1}$ . Typical values are provided, with coverage factor  $k=1$ , corresponding to one standard deviation  $1\sigma$ .
- Systematic uncertainty associated to the estimation of molecular density/extinction profile  $U_{p,T}$ .  
 $U_{p,T}$  : < 10% for  $\alpha(z) > 2 \times 10^{-5} \text{m}^{-1}$ ; > 10% for  $\alpha(z) < 2 \times 10^{-5} \text{m}^{-1}$ . Uncertainty values based on the sensitivity of the extinction coefficient retrieval at 532 nm to the air density profile, considering as a reference the air density profile obtained from temperature and pressure profiles measured with radiosoundings [28,29].
- Systematic uncertainty associated to the Ångström exponent assumption  $U_{\text{Å}}$   
 $U_{\text{Å}}$ : < 5%. Uncertainty value based on the sensitivity of the extinction coefficient retrieval at 532 nm to the Ångström exponent assumption [28,30].
- Total maximum systematic uncertainty  $U_{\text{sys}}^{\text{max}} = U_{p,T} + U_{\text{Å}}$  : < 15% for  $\alpha(z) > 2 \times 10^{-5} \text{m}^{-1}$ ; > 15% for  $\alpha(z) < 2 \times 10^{-5} \text{m}^{-1}$

Assuming the total maximum systematic uncertainty  $U_{\text{sys}}^{\text{max}}$  as a normal random uncertainty with coverage factor  $k = 3$  ( $3\sigma$ ), the total uncertainty for  $k = 2$  ( $2\sigma$ ), resulting from the combination of  $U_{\text{sys}}^{\text{max}}$  and  $U_{\text{stat}}$ , is given by:

$U_{\text{tot}} = [(2/3U_{\text{sys}}^{\text{max}})^2 + (2U_{\text{stat}})^2]^{1/2}$ , giving typical uncertainties less than 23% for  $\alpha(z) > 2 \times 10^{-5} \text{m}^{-1}$  and higher than 23% for  $\alpha(z) < 2 \times 10^{-5} \text{m}^{-1}$ .

## 7 Traceability uncertainty analysis

Traceability level definition is given in Table 1.

**Table 1. Traceability level definition table**

Traceability Level	Descriptor	Multiplier
High	SI traceable or globally recognised community standard	1
Medium	Developmental community standard or peer-reviewed uncertainty assessment	3
Low	Approximate estimation	10

Analysis of the summary table would suggest the following contributions, shown in Table 2, should be considered further to improve the overall uncertainty of the EARLINET aerosol extinction coefficient product. The entries are given in an estimated priority order.

**Table 2. Traceability level definition further action table.**

Element identifier	Contribution name	Uncertainty contribution form	Typical value	Traceability level (L/M/H)	random, structured random, quasi-systematic or systematic?	Correlated to? (Use element identifier)
7a	Molecular density and extinction profile	equation (3) for the retrieval of aerosol extinction coefficient profile	< 10% for $\alpha(z) > 2 \times 10^{-5} \text{ m}^{-1}$ > 10% for $\alpha(z) < 2 \times 10^{-5} \text{ m}^{-1}$	M	systematic	none
7b	Ångström exponent assumption	equation (3) for the retrieval of aerosol extinction coefficient profile	< 5%	M	systematic	none
3	Detectors	N/A	0 %	M	systematic	none
6h	Overlap correction	N/A	0% for $z > z_{\text{ovl}}/z_0$ up to 50% for $z < z_{\text{ovl}}/z_0$	M	systematic	none
7d	Retrieval of aerosol extinction	Poiss/norm distribution	<10% ( $1\sigma$ ) for $\alpha(z) > 2 \times 10^{-5} \text{ m}^{-1}$	M	random	5, 6b, 6d, 6e, 6f & 6g

	coefficient profile		$>10\%(1\sigma)$ for $\alpha(z) < 2 \times 10^{-5} \text{m}^{-1}$			
1	Transmission system	N/A	0 %	M	systematic	none
2a	Receiver optical parameters	N/A	0 %	M	systematic	none
2b	Alignment of the lidar system	N/A	0 %	M	systematic	none
6a	Dead time correction	N/A	0 %	M	systematic	4
6b	Dark subtraction	N/A	0 %	M	systematic	4
6c	First range bin/Trigger delay correction	N/A	0 %	M	systematic	4
6d	Background subtraction	N/A	0 %	M	systematic	4
7c	Multiple scattering correction	N/A	0 %	M	systematic	none

## 7.1 Recommendations

- ✓ The systematic uncertainty associated to the estimation of molecular density/extinction profile (7a) can be reduced by using pressure and temperature profiles measured with co-located and simultaneous radio-soundings, if available, or provided by NWP re-analysis.
- ✓ Both uncertainty contributions (7a) and (7b), based on sensitivity studies performed on specific measurement sessions and lidar systems, could potentially be improved by extending the sensitivity studies to multiple measurements and lidar systems and by making uniform the methodologies to estimate both the molecular density profile and the Ångström exponent.
- ✓ An assessment of the uncertainty of the detector efficiency (3), due to the spatial inhomogeneities of its photocathode and to the variations of its quantum efficiency, should be evaluated.
- ✓ The experimental determination of overlap function for all the systems in the network can improve the uncertainty contribution of overlap correction (6h) below  $Z_{ovl}/Z_0$ .
- ✓ The random uncertainty (7d) could potentially be improved by making uniform all applied signal handling procedures both in pre-processing and processing stages: dark subtraction, background subtraction, binning, temporal integration, signal gluing and the calculus of aerosol extinction coefficient  $\alpha(z)$  by equation (3), including a vertical smoothing.

- ✓ Finally, there are eight contributions that do not have an assigned uncertainty. Some analysis to determine the magnitude of these potential contributions would better constrain the uncertainty budget.

## 8 Conclusion

The EARLINET lidar aerosol extinction coefficient product has been assessed against the GAIA CLIM traceability and uncertainty criteria.

## 9 References

1. G. Pappalardo, A. Amodeo, A. Apituley, A. Comeron, V. Freudenthaler, H. Linné, A. Ansmann, J. Bösenberg, G. D'Amico, I. Mattis, L. Mona, U. Wandinger, V. Amiridis, L. Alados-Arboledas, D. Nicolae, and M. Wiegner: EARLINET: towards an advanced sustainable European aerosol lidar network, *Atmos. Meas. Tech.*, 7, 2389–2409, <https://doi.org/10.5194/amt-7-2389-2014>, 2014.
2. D'Amico, G., Amodeo, A., Mattis, I., Freudenthaler, V., and Pappalardo, G.: EARLINET Single Calculus Chain – technical – Part 1: Pre-processing of raw lidar data, *Atmos. Meas. Tech.*, 9, 491–507, doi:10.5194/amt-9-491-2016, 2016.
3. Mattis, I., D'Amico, G., Baars, H., Amodeo, A., Madonna, F., and Iarlori, M.: EARLINET Single Calculus Chain – technical – Part 2: Calculation of optical products, *Atmos. Meas. Tech.*, 9, 3009–3029, doi:10.5194/amt-9-3009-2016, 2016.
4. N. Papagiannopoulos, L. Mona, L. Alados-Arboledas, V. Amiridis, H. Baars, I. Biniotoglou, D. Bortoli, G. D'Amico, A. Giunta, J. L. Guerrero-Rascado, A. Schwarz, S. Pereira, N. Spinelli, U. Wandinger, X. Wang, and G. Pappalardo: CALIPSO climatological products: evaluation and suggestions from EARLINET, *Atmos. Chem. Phys.*, 16, 2341–2357, doi:10.5194/acp-16-2341-2016, 2016.
5. Wandinger, U., Freudenthaler, V., Baars, H., Amodeo, A., Engelmann, R., Mattis, I., Groß, S., Pappalardo, G., Giunta, A., D'Amico, G., Chaikovsky, A., Osipenko, F., Slesar, A., Nicolae, D., Belegante, L., Talianu, C., Serikov, I., Linné, H., Jansen, F., Apituley, A., Wilson, K. M., de Graaf, M., Trickl, T., Giehl, H., Adam, M., Comeron, A., Muñoz-Porcar, C., Rocadenbosch, F., Sicard, M., Tomás, S., Lange, D., Kumar, D., Pujadas, M., Molero, F., Fernández, A. J., Alados-Arboledas, L., Bravo-Aranda, J. A., Navas-Guzmán, F., Guerrero-Rascado, J. L., Granados-Muñoz, M. J., Preißler, J., Wagner, F., Gausa, M., Grigorov, I., Stoyanov, D., Iarlori, M., Rizi, V., Spinelli, N., Boselli, A., Wang, X., Lo Feudo, T., Perrone, M. R., De Tomasi, F., and Burlizzi, P.: EARLINET instrument intercomparison campaigns: overview on strategy and results, *Atmos. Meas. Tech.*, 9, 1001–1023, doi:10.5194/amt-9-1001-2016, 2016.
6. P. Sawamura, J. P. Vernier, J. E. Barnes, T. A. Berkoff, E. J. Welton, L. Alados-Arboledas, F. Navas-Guzman, G. Pappalardo, L. Mona, F. Madonna, D. Lange, M. Sicard, S. Godin-Beekmann, G. Payen, Z. Wang, S. Hu, S. N. Tripathi, C. Cordoba-Jabonero and R. M. Hoff: Stratospheric AOD after the 2011 eruption of Nabro volcano measured by lidars over the Northern Hemisphere,

Environ. Res. Lett., 7, 034013, doi:10.1088/1748-9326/7/3/034013, 2012.

7. EARLINET ASOS NA3 Quality Assurance webpage at [https://www.meteo.physik.uni-muenchen.de/~stlidar/earlinet\\_asos/EARLINET-ASOS-NA3-QA.html](https://www.meteo.physik.uni-muenchen.de/~stlidar/earlinet_asos/EARLINET-ASOS-NA3-QA.html).
8. V. Simeonov, G. Larcheveque, P. Quaglia, H. Van Den Bergh, and B. Calpini: Influence of the Photomultiplier Tube Spatial Uniformity on Lidar Signals, *Appl. Opt.* 38, 5186-5190, 1999.
9. Freudenthaler, V., Effects of spatially inhomogeneous photomultiplier sensitivity on lidar signals and remedies, Proceedings of the 22nd International Laser Radar Conference (ILRC 2004), Matera, Italy, 12-16 July, ESA Publications Division, SP-561, 37-40, 2004.
10. Evans, R. D.: *The Atomic Nucleus*, McGraw-Hill, New York, chapter 28, 785–794, 1955.
11. F. A. Johnson, R. Jones, T. P. McLean, and E. R. Pike: Dead-time corrections to photon counting distributions, *Phys. Rev. Lett.*, 16, N. 13, pp. 589-592, 1966.
12. Whiteman, D. N., Melfi, S. H., and Ferrare, R. A.: Raman lidar system for the measurement of water vapor and aerosols in the Earth's atmosphere, *Appl. Opt.*, 31, 3068–3082, 1992.
13. Freudenthaler, V., Linné, H., Chaikovsky, A., Groß, S., and Rabus, D.: Internal quality assurance tools, *Atmos. Meas. Tech. Discuss.*, in preparation, 2016.
14. Amodeo, A., Statistical error evaluation in aerosol optical properties retrieval, 5th EARLINET-ASOS workshop -Training course, Thessaloniki, 25 – 26 February 2008, available at <https://www.earlinet.org/index.php?id=66>
15. Whiteman, D. N., Demoz, B., Rush, K., Schwemmer, G., Gentry, B., Di Girolamo, P., Comer, J., Veselovskii, I., Evans, K., Melfi, S. H., Wang, Z., Cadirola, M., Mielke, B., Venable, D., and Van Hove, T.: Raman Lidar Measurements during the International H2O Project. Part I: Instrumentation and Analysis Techniques, *J. Atmos. Oceanic Tech.*, 23, 157–169, 2006.
16. Newsom, R. K., Turner, D. D., Mielke, B., Clayton, M., Ferrare, R., and Sivaraman, C.: Simultaneous analog and photon counting detection for Raman lidar, *Appl. Opt.*, 48, 3903–3914, 2009.
17. Walker, M., Venable, D., and Whiteman, D. N.: Gluing for Raman lidar systems using the lamp mapping technique, *Appl. Opt.*, 53, 8535–8543, 2014.
18. Kuze, H., H. Kinjo, Y. Sakurada, and N. Takeuchi, Field-of-view dependence of lidar signals by use of Newtonian and Cassegrainian telescopes, *Appl. Opt.*, 37, 3128–3132, 1998.
19. Measures, R. M., *Laser remote sensing: fundamentals and applications*, 2 ed., 510 pp., Krieger Publishing Company, Malabar, Florida, 1992.
20. Chourdakis, G., A. Papayannis, and J. Porteneuve, Analysis of the receiver response for a noncoaxial lidar system with fiber-optic output, *Appl. Opt.*, 41, 2715–2723, 2002.
21. Wandinger, U., and A. Ansmann, “Experimental determination of the lidar overlap profile with Raman lidar”, *Appl. Opt.*, 41, 511–514, 2002.

22. Freudenthaler, V., Handbook of instruments, Tech. rep., EARLINET ASOS, 2007.
23. Ansmann, A., M. Riebesell, and C. Weitkamp, "Measurements of atmospheric aerosol extinction profiles with Raman lidar", *Optics Letters* 15, 746-748, 1990.
24. Pappalardo G., A. Amodeo, M. Pandolfi, U. Wandinger, A. Ansmann, J. Bosenberg, V. Matthias, V. Amiridis, F. De Tomasi, M. Frioud, M. Iarlori, L. Komguem, A. Papayannis, F. Rocadenbosch, and X. Wang, "Aerosol lidar intercomparison in the framework of the EARLINET, project. 3. Raman lidar algorithm for aerosol extinction, backscatter and lidar ratio", *Appl. Opt.*, 43(28), 5370–5385, 2004.
25. Iarlori, M., Madonna, F., Rizi, V., Trickl, T., and Amodeo, A.: Effective resolution concepts for lidar observations, *Atmos. 20 Meas. Tech.*, 8, 5157-5176, doi:10.5194/amt-8-5157-2015, 2015.
26. A. Bucholtz, Rayleigh-scattering calculations for the terrestrial atmosphere, *Appl. Opt.* Vol. 34, N. 15, pp. 2765-2773 (1995).
27. R. Miles et al, Laser Rayleigh scattering, *Meas. Sci. Technol.* , 12, R33-R51 (2001).
28. Ansmann, A., U. Wandinger, M. Riebesell, C. Weitkamp, and W. Michaelis, Independent measurement of extinction and backscatter profiles in cirrus clouds by using a combined Raman elastic-backscatter lidar, *Appl. Opt.*, 31, 7113–7131, 1992.
29. Mattis, I., Retrieval of aerosol optical properties, 5th EARLINET-ASOS workshop -Training course, Thessaloniki, 25 – 26 February 2008, available at <https://www.earlinet.org/index.php?id=66>
30. Ansmann, A. and Müller, D., "Lidar and atmospheric aerosol particles", in: *LIDAR – Range-resolved optical remote sensing of the atmosphere*, edited by: Weitkamp, C., Springer, New York, USA, 105–141, 2005.
31. Wandinger, U., "Multiple-scattering influence on extinction and backscatter coefficient measurements with Raman and high-spectral resolution lidars", *Applied Optics*, Vol.37, N.3, 417 - 427, 1998.
32. Eloranta, E.E., "Practical model for the calculation of multiply scattered lidar returns", *Applied Optics*, Vol.37, N.12, 2464 – 2472, 1998.
33. I. Mattis, A. Chaikovsky, A. Amodeo, G. D'Amico, and G. Pappalardo: Assessment report of existing calculus subsystems used within EARLINET-ASOS, available at <http://wiki.tropos.de/images/7/7a/Subsystems.pdf>, April 1, 2007.

